

Immersive and Wearable Thermal Rendering for Augmented Reality

Alexandra Watkins^{1,*}, Ritam Ghosh², Evan Chow¹, and Nilanjan Sarkar^{1,2}

¹Vanderbilt University, Mechanical Engineering, Nashville, 37212, USA

²Vanderbilt University, Electrical and Computer Engineering, Nashville, 37212, USA

*alexandra.watkins@vanderbilt.edu

ABSTRACT

In augmented reality (AR), where digital content is overlaid onto the real world, realistic thermal feedback has been shown to enhance immersion. Yet current thermal feedback devices, heavily influenced by the needs of virtual reality, often hinder physical interactions and are ineffective for immersion in AR. To bridge this gap, we have identified three design considerations relevant for AR thermal feedback: indirect feedback to maintain dexterity, thermal passthrough to preserve real-world temperature perception, and spatiotemporal rendering for dynamic sensations. We then created a unique and innovative thermal feedback device that satisfies these criteria. Human subject experiments assessing perceptual sensitivity, object temperature matching, spatial pattern recognition, and moving thermal stimuli demonstrated the impact of our design, enabling realistic temperature discrimination, virtual object perception, and enhanced immersion. These findings demonstrate that carefully designed thermal feedback systems can bridge the sensory gap between physical and virtual interactions, enhancing AR realism and usability.

1 Introduction

Thermal sensations, though frequently taken for granted, play a vital role in crafting realistic experiences within immersive synthetic environments such as virtual reality (VR) and augmented reality (AR). Accurately conveying sensations of warmth and coolness can significantly enhance users' sense of presence, interactivity, and immersion²⁻⁴. The need for such methods to increase immersion and the overall experience of the user is rapidly growing, as immersive technologies, particularly AR, are becoming increasingly prevalent in diverse fields, including education, training of the workforce, and industrial processes⁵⁻⁷. The effectiveness of these applications depends greatly on their fidelity—the realism and engagement they provide—leading to improved learning outcomes⁸⁻¹⁰. By fostering immersion in specific scenarios, these technologies encourage sustained attention, usability, and user enjoyment¹¹.

The critical role of accurate thermal feedback stems directly from the integral part thermal cues play in our daily lives. Everyday interactions, such as holding a hot beverage or gripping a cold metal rail, profoundly shape our perceptions of safety, comfort, and material identification. These routine experiences are mediated by thermoreceptors in the skin, which detect temperature variations and initiate rapid behavioral responses¹. This continuous interplay between skin temperature and environmental stimuli is essential for interpreting surface properties, detecting temperature gradients, and experiencing transitions between different environments. Effectively integrating these sensory experiences into immersive technologies can significantly enhance realism and user engagement.

1.1 Augmented Reality and the Impact of Haptic Feedback

Augmented Reality refers to a group of technologies that overlay digital information, such as images, videos, or sounds, onto the real world^{12,13}. AR blends these virtual elements into the user's surrounding environment, enhancing the way we perceive our surroundings. This means that, in contrast to VR technologies, the AR user is still able to see and interact with the real world around them to a varying degree depending on the level of virtuality introduced by the system.

AR systems have become remarkably sophisticated in their visual and audio fidelity in recent years, driven by advances in head-mounted displays (HMDs) like the Microsoft HoloLens 2¹⁴ and the Apple Vision Pro¹⁵. But is an HMD's purely visual/aural feedback sufficient for immersive AR experiences? Recent studies suggest otherwise, calling out the need for new methods of incorporating visuo-haptic feedback to create more immersive AR applications¹⁶⁻¹⁸. Appropriate feedback increases the perceived presence of remote users and objects, leading to more effective human-human and human-machine interaction¹⁹. Haptic feedback can even increase task focus and performance, with better immersion giving users a better outlook on AR applications^{16,20}.

1.2 Immersive Thermal Feedback

Although force feedback technologies have matured considerably—ranging from exoskeleton gloves to grounded force-feedback arms—an often underexplored but vital dimension of haptics is thermal feedback². Studies show that even rudimentary thermal sensations can boost perceived realism by mimicking real-world interactions^{1,21}, and if a virtual object provides the same thermal response as its real counterpart it is more easily perceived as present within a user’s environment²². Beyond object interactions, the inclusion of thermal sensations as directional cues or to augment the transition between environments has been shown to provide stronger feelings of immersion and presence².

Early investigations into thermal feedback have focused predominantly on VR. Researchers have experimented with methods such as infrared heating²³, chilled air jets²⁴, and wearable devices that impart temperature changes to the skin^{2,25,26}. Many of these approaches can replicate simple temperature gradients and are compatible with fully virtual environments, where the user’s interactions are confined to simulated objects and spaces.

However, these techniques often occlude or restrict the user’s natural sense of touch when handling real objects. Handheld controllers that double as thermal devices can interfere with dexterity²⁷, while glove-based solutions may add considerable bulk and reduce tactile sensitivity to real-world surfaces. Additionally, many commercial devices developed for research or consumer use incorporate thermal feedback alongside other modalities of feedback, such as HaptX’s (<https://haptx.com>) line of exoskeleton gloves that utilize microfluid channels and actuators to render both changes in temperature and tactile cues. These methods of multi-modal feedback add further complexity and bulk to wearable devices, exacerbating challenges in sensing and manipulating physical components of the environment. Although these compromises may be acceptable in purely virtual contexts, they become problematic in scenarios where the user needs to interact fluidly with both physical and virtual entities, as is the case in AR. These restrictions on interacting with both real and virtual objects often make it impractical to utilize current thermal devices when operating within an augmented workspace. There is a need for clearly identified and defined design considerations that future devices can utilize to develop thermal feedback technology specifically for AR.

AR’s blending of physical and virtual environments imposes special constraints on thermal feedback devices. Ideally, such devices should be capable of:

- *preserving the user’s ability to sense real-world temperatures, and*
- *allowing unobstructed and untethered manipulation of physical objects, while simultaneously*
- *providing localized warmth or coolness that emulates contact with virtual elements, and*
- *accurately depicting changes in surface contact and transitions in the environment*

Current technologies do not fully meet these capabilities. Designs that aim to cover the user’s fingertips or palms entirely can diminish the user’s natural thermal perception of real objects and limit hand movements. Stationary systems such as infrared lamps or chilled air nozzles may only be effective in small work volumes, restricting user mobility^{23,24}. As a result, there is a need for thermal feedback solutions specifically tailored to AR scenarios, where haptic fidelity and unimpeded real-world contact are both essential.

1.3 Present Work

In this work, we present a set of three design considerations (DCs) for developing thermal feedback technologies for immersive mixed/augmented reality experiences. These considerations are meant to be additional capabilities or constraints to be kept in mind when developing a device for AR. The first two considerations deal with minimizing the impact of a thermal feedback device on the user’s ability to interact with their physical environment. The last consideration details additional capabilities we believe necessary to allow virtual elements of the environment to naturally blend with the user’s physical environment.

DC 1: Utilize indirect feedback

DC 2: Incorporate thermal passthrough of real-world temperatures

DC 3: Provide spatiotemporal renderings of thermal sensations

We then present and evaluate a novel wearable thermal feedback device that satisfies all three considerations (Figure 1). Our device consists of an innovative array of thermoelectric modules (TEMs) arranged in a 3x3 grid on the palm. Each module functions as an individual heat pump, capable of independently adjusting its temperature to render spatially and temporally varying thermal patterns. A 10k Ω thermistor was fused to the active surface of each TEM for closed loop control. Each TEM-Thermistor assembly was mounted on a 10mmx10mm aluminum plate and embedded within a flexible silicone base, with internal water-cooling channels preventing thermal buildup by managing the temperature of the aluminum base plate acting as a

heat sink. A 3x3 array of thermistors on the outward facing external surface of the silicone base allows the device to measure the temperature of contacted surfaces to enable the passthrough of physical object thermal properties even when the palm is obstructed.

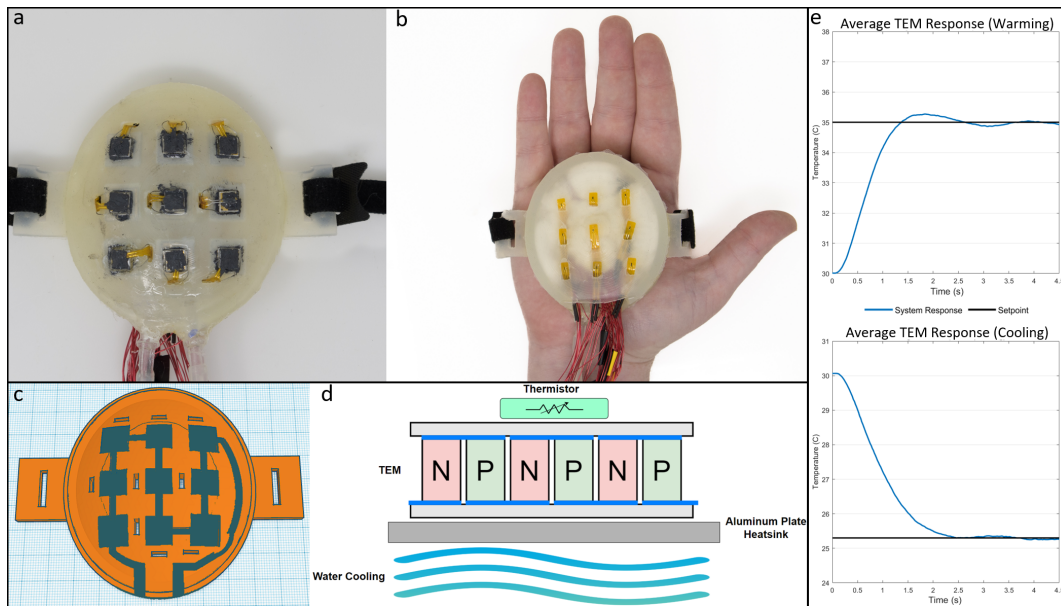


Figure 1. Overview of the proof-of-concept wearable thermal feedback system.

(a) Thermal feedback is applied by an array of individually controlled Peltier devices (thermoelectric modules) with temperature feedback from thermistors mounted to each contact surface. (b) Outward-facing thermistors allow for measurement of contact surface temperatures for thermal passthrough. (c) Interior to the silicone base is a water-cooling channel for temperature management. (d) A single thermal actuation unit consists of a TEM and thermistor mounted on an aluminum base that acts as a water-cooled heatsink. (e) The average temperature response to a step input while in contact with a human palm with an ambient temperature of 30°C.

We chose to mount the device against the user’s palm as we believe the palm of the hand is a prime candidate for a relocation target that satisfies **DC 1: Indirect Feedback**. The palm is still near the contact surfaces of the fingers, can be a direct point of contact with virtual objects itself, and provides a relatively large surface area in which to render thermal sensations. Additionally, recent work has investigated the sensitivity of the palm and shown that it is sufficient for thermal cues^{28,29}.

We make use of the large surface area of the palm by incorporating an array of 6.5mmx6.5mm thermoelectric modules (CUI Device CP076581-238P) arranged in a 3x3 grid with 18mm spacing. This multi-actuator design has been shown by previous studies to be a reliable method of thermal rendering. Zhipeng et al.³⁰ developed a thermal display composed of a 3x3 set of heating actuators and a single thermoelectric module for cooling. More recently, a wearable 4x4 array of thermoelectric actuators was developed by Li et al. for use in hand rehabilitation of stroke victims³¹. A more complex application of an array of thermal actuators is seen in the work by Kim et al.³², where a two-dimensional array of thermoelectric modules was integrated into the handle of a blind-assistive cane. However, there is currently no work utilizing such an array for thermal feedback in AR.

The individual modules are encapsulated within a flexible silicone base, a material chosen for its excellent mechanical flexibility and bio-compatibility. The flexibility and lightness of this material allows the device to be worn unobtrusively on the palm while the user explores their environment. We made use of a two-part mold fabrication process to create interior water-cooling channels, designed to disperse heat away from the TEMS to avoid reducing efficiency during heavy or sustained operation due to thermal losses. The current device prototype is restricted in movement only due to the stationary control circuitry and water cooling reservoir necessary for the device. Furthermore, by snugly fitting into the user’s palm, the flexible nature of the device allows the array to contour to the unique topography of each user’s palm, promoting efficient heat transfer. This contouring effect is enhanced by securely strapping the device to the hand, applying significant contact pressure and reducing the likelihood of positional slippage during movement.

Through a series of human subjects experiments (N=12), we show that targeting thermally sensitive areas of the palm for indirect feedback, enabling passthrough of real-world temperatures, and rendering spatiotemporal patterns of warmth or coolness can enhance the sense of immersion in AR experiences. The first human subjects experiment measured the

Just-Noticeable-Difference (JND) of the device, verifying its ability to provide sufficient thermal feedback. The utility of incorporating a temperature passthrough system into the device to render thermal properties of physical objects on occluded areas of the skin was verified in our second experiment, where participants interacted with both real and virtual objects. We measured both the accuracy in identifying similar/dissimilar temperatures between real and virtual objects as well as collected open-ended feedback from participants about their experience. Two experiments were conducted to assess the impact of spatiotemporal rendering. First the ability to recognize discrete spatial patterns was assessed by asking participants to discriminate between pairs of thermal patterns presented using the device's thermal array. Finally, to validate the ability to display moving spatiotemporal patterns, an experiment integrating the device within an AR experience was conducted, wherein a post-experience questionnaire collected qualitative data on use experience and the perceived realism of thermal movement. The results of these experiments not only demonstrate that our novel device is capable of meeting all of our additional AR design considerations, but also present both quantitative and qualitative data suggesting that meeting these additional criteria leads to more realistic and immersive AR experiences.

2 Results

2.1 Design considerations for Mixed/Augmented Reality

When designing a thermal haptic feedback device for AR applications, the primary goal is to achieve an optimal balance between maintaining real-world thermal perception and enhancing the perception of virtual elements in order to create an immersive experience (Figure 2). The device must ensure that interactions with the physical environment remain natural and intuitive by minimizing the interference it causes with the real world. Simultaneously, it must provide sufficient and realistic thermal cues during virtual interactions to instill the sensation of embodiment and presence for virtual objects. This balance is crucial, as it allows users to navigate between physical and virtual worlds without a disruptive sensory experience. This section details the identification of three specific design considerations we believe must be considered when developing a thermal haptic device intended for use in AR. The first two considerations pertain to maintaining the authenticity of perceiving physical objects, while the last consideration addresses methods of rendering thermal sensations necessary to maintain parity between real and virtual objects.

2.1.1 DC 1: Utilize indirect feedback

We begin deriving our design considerations by considering how to preserve common methods of touch interactions in AR. A recent work by Bhatia, Hornbæk, and Seifi³³ identified four types of touch interactions commonly used in AR from the set of exploratory procedures previously defined by Lederman and Klatzky³⁴. Of these four types, three require the use of the thumb or fingers. As such, a practical solution to meeting the needs of AR environmental interactions is to *apply thermal feedback in a different location than the actual point of contact*. By doing so, the user can directly touch and manipulate physical objects unencumbered, while still perceiving temperature changes that correspond to the virtual environment. This concept of *indirect feedback* has been shown to be viable in several forms, including retargeting thermal stimuli to the base of the finger³⁵ or to the user's wrist³⁶.

Thermal feedback is commonly used in state-of-the-art multi-modal devices but often results in bulky designs that hinder user dexterity. However, addressing this issue by moving the thermal actuators and the point of feedback away from the fingertips introduces an additional challenge: As the thermal actuators become smaller or are positioned in areas out of the way, they may deliver or remove less heat to the skin, reducing the user's ability to perceive feedback. Even devices specifically optimized for rendering thermal sensations tend to rely on covering large skin areas, exacerbating encumbrance. Reducing actuator size can alleviate these mobility concerns but diminishes the overall power output and contact area, which in turn lessens the perceived intensity of the thermal stimulus³⁷.

To overcome these limitations while preserving effective thermal feedback, we propose focusing on *sensitive skin regions* when implementing indirect feedback. Thermal perception is mediated by free nerve endings known as thermoreceptors, which respond to changes in skin temperature³⁸. Two distinct receptor systems detect warm and cold sensations, with cold receptors generally outnumbering warm receptors, thereby contributing to heightened cold sensitivity. Filingeri et al.²⁸ further demonstrated that sensitivity varies across different parts of the body, while Caldwell et al.³⁹ have shown that thermoreceptors respond dynamically to both absolute and rate-based temperature changes. By strategically positioning smaller, low-power actuators on areas with a higher thermoreceptor density or greater thermal sensitivity, we believe designers can maintain a significant thermal effect without sacrificing the user's dexterity or comfort.

2.1.2 DC 2: Incorporate thermal passthrough

The last type of common AR touch interaction identified by Bhatia et al. is static contact and holding, where users maintain sustained touch with an object or surface. This method of interaction is particularly important for perceiving thermal properties of the environment, as humans intuitively use various regions of their skin, such as the palms, fingers, or even forearms, to

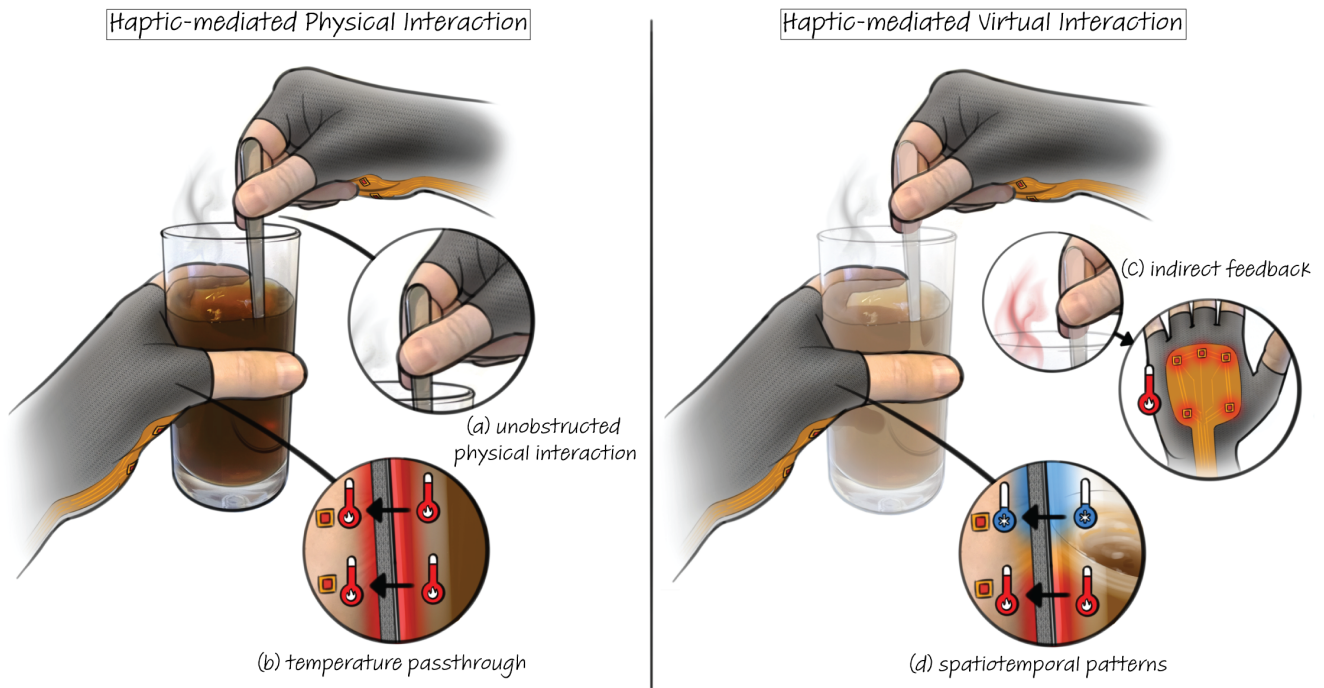


Figure 2. Haptic-mediated thermal interactions in AR enabled by derived design considerations.

(a) *Physical Interaction*. The lack of actuators on the fingers allows for fine manipulation of physical tools or other objects. Direct thermal sensing of contact surfaces is possible due to no occlusion. (b) *Physical Interaction*. Temperature sensors on the external surface of a haptic device allow collocated thermal actuators on its interior surface to mimic the thermal properties of contacted surfaces. This maintains the thermal sensing capabilities of regions of the body occluded by the device. (c) *Virtual Interaction*. Thermal sensations applied to nearby occluded regions in sync with the actions of the user can maintain the perception of thermal sensing even when actuators are not present on the fingers. (d) *Virtual Interaction*. Independently controlled and spatially arranged thermal actuators enable the presentation of sensations that vary both across a contact surface and with time. In this case, the interior surface of a virtual cup being covered and subsequently uncovered by splashes of a warm liquid is represented by a spatially and temporally dynamic sensation on the palm.

gather thermal cues. However, when a thermal feedback device that requires contact is placed on these sensitive regions, it blocks direct contact with the physical environment. This creates a challenge: the user is no longer able to feel the true thermal characteristics of the object they are holding, potentially diminishing their sense of immersion and realism. Simply utilizing indirect feedback by itself does not adequately address this, as there is still the possibility the area of skin occluded by the device is needed for intuitive interactions. To address this issue, we propose that a thermal feedback device must *incorporate thermal passthrough*, wherein the device measures the thermal properties of a physical object's surface when contact is made with the device and subsequently renders these sensations to the user. By doing so, the device can restore the lost thermal interaction with the real-world object, maintaining immersion without sacrificing the benefits of the thermal feedback system. This approach allows users to explore and interact with the environment naturally while still benefiting from the augmented thermal feedback provided by the device.

2.1.3 DC 3: Provide spatiotemporal renderings of thermal sensations

A key challenge in creating immersive AR experiences is replicating the thermal complexity that characterizes real-world objects and environments. This complexity comprises both *spatial* variations in temperature across a surface and *temporal* changes that occur when an object or user is in motion. Although many devices deliver only a single, uniform temperature or limited directional cues, high-fidelity experiences demand greater nuance in how temperature is rendered.

Spatially Varying Thermal Patterns. As AR users interact with both real and virtual objects, immersion can be disrupted if certain sensory modalities essential for physical exploration are absent in their virtual counterparts. Thermal sensations, for example, play a critical role in interpreting surface patterns and variations⁴⁰. Consequently, virtual elements must not only reproduce absolute temperatures but also capture the spatial differences that would be encountered on a physical object's surface. This parallels the lateral motion and contour-following techniques identified by Lederman and Klatzky³⁴, where dynamic touch interactions reveal textures and shapes, thereby highlighting the need for spatially dynamic thermal feedback.

Despite its importance, rendering spatially varying thermal patterns remains underexplored. Most existing applications restrict thermal cues to a single area or rely on multiple discrete sources primarily for directional hints or increasing contact area. However, a device capable of detailed, spatially varying thermal patterns is vital for achieving parity between physical and virtual objects. Bench-top systems designed for thermal tactile sensation⁴⁰ and wearable skin-like actuators⁴¹ demonstrate the potential for such feedback. Nevertheless, these solutions are often bulky or specialized for laboratory settings, leaving a gap for compact, highly mobile devices optimized for AR applications.

Temporal Variations and Moving Thermal Illusions. Equally important to the sense of realism is the dynamic, *time-varying* dimension of thermal feedback. Users rarely keep their hands static: they move them along surfaces or even grasp objects in motion. For example, in collaborative AR scenarios the user might shake hands with a virtual avatar representing a remote user, or reach out and touch the avatar's arm as part of a social interaction. Replicating these motion-based interactions requires capturing how a temperature distribution *changes over time*.

Existing approaches often combine a static thermal source with vibrotactile cues to create the illusion of moving heat or cold. The phenomenon of thermal referral⁴² is often leveraged: a stationary thermal stimulus appears to move when combined with a shifting vibration. Liu et al.⁴³ exploited this illusion by overlaying static thermal output with a moving tactile sensation, while Son et al.⁴⁴ developed a vest incorporating vibrotactile and thermal actuators to render moving thermal sensations. Nakatani et al.⁴⁵ similarly used a low-resolution grid of thermoelectric modules alongside a higher-resolution vibrotactile matrix to achieve a sense of thermal motion.

However, an alternative option is to render spatio-temporal patterns *solely using thermal actuators*. By arranging multiple closely spaced actuators in a grid and activating them in sequence, one can induce a “thermal brush” effect akin to vibrotactile illusions of motion⁴⁶. We believe that staggering the onset of thermal stimuli along a line or grid of actuators should enable users to perceive a single, continuously moving thermal source. Although such purely thermal-based illusions have yet to be widely explored, their successful implementation would further enhance immersion by allowing complex, dynamic temperature profiles to be fully integrated into AR objects—no additional modality required.

In summary, designing thermal feedback for AR calls for balancing real-world interactivity with the augmentation of virtual elements. The first consideration, *indirect feedback*, ensures that users can continue to manipulate physical objects naturally by relocating thermal stimulation to less obstructive areas and targeting highly sensitive skin regions. *Thermal passthrough* then restores critical contact-based temperature cues from real-world surfaces by actively conveying these properties through the device. Finally, *spatiotemporal rendering* enables complex thermal sensations that capture both the spatial variation of temperatures across surfaces and the dynamic changes resulting from user or object motion.

2.2 Thermal Device Assessment

It is important to ensure that the low power actuators used in the thermal device are capable of rendering an appropriate range of temperatures when in contact with the user's skin. Additionally, to provide meaningful feedback, it must incorporate the

thermal response times observed for both warm and cold sensations and consider the temperature range in which each type of thermoreceptor is activated.

Characterization tests show the device’s operational temperature range spans 15°C above and below the user’s ambient skin temperature, with onset temperature change rates exceeding $0.1 \frac{^{\circ}\text{C}}{\text{s}}$. As humans are sensitive not only to temperature differentials but also the rate of temperature change⁴⁷, the device’s rapid initial rate of change of temperature allows for rendered thermal sensations to have similar response times as thermal sensing using natural skin contact. A more detailed description of the performance of the device is provided in Section 4: Methods.

2.3 Participants

Twelve (12) individuals from Vanderbilt University’s undergraduate and graduate student populations were recruited for this study. Recruitment focused on participants who were available during the study’s scheduled sessions and willing to take part. Prior to participation, each individual was provided with a detailed explanation of the study’s purpose, procedures, potential risks, benefits, and their rights as participants. Written informed consent was obtained after participants had the opportunity to ask questions and receive clarification.

Each participant attended four sessions, lasting one hour each, during which they completed the study’s tasks and activities. This session length was chosen to balance data collection needs with minimizing participant fatigue or discomfort.

The participant group had a median age of 24.2 years with a standard deviation of 3.4 years. Most participants reported minimal or no prior experience with head-mounted display (HMD) VR/AR technology.

2.4 Experiment 1: JND Testing

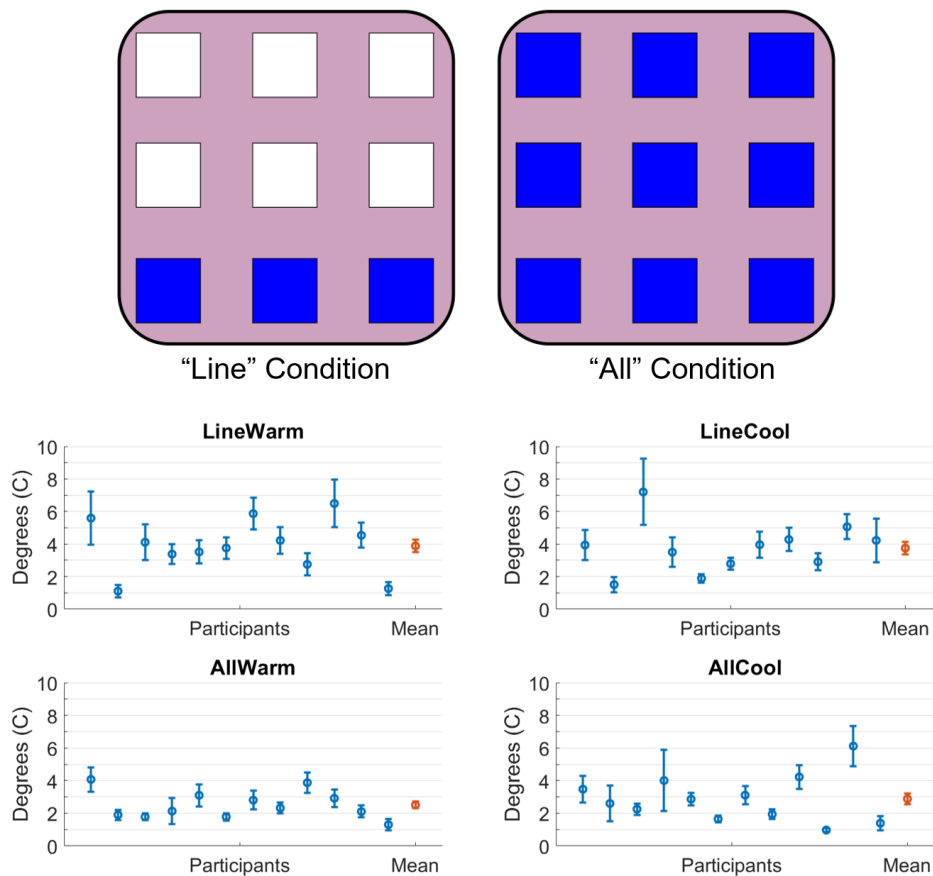


Figure 3. Just Noticeable Difference (JND) Experiment Conditions and Results Two distinct spatial patterns were applied to the device for both heating and cooling JND calculations. (*Line*) The "Line" pattern activated bottom row of TEMs on the device. (*All*) For the "All" pattern, all TEMs were activated. (*JND Results*) The JND (in degrees celsius) quantifies the smallest change in a reference temperature that is detectable with a 75% confidence. Per-participant JND is shown in blue and the overall JND is shown in orange.

We must ensure that the device does not impede the user's natural aptitude in sensing thermal stimuli. As such, we quantified the Just Noticeable Difference (JND) related to the thermal device. The JND represents the smallest discernible variation in magnitude between a reference stimulus and a test stimulus that a human can identify with a specific degree of reliability. For our experiment, we computed the JND at the 75% threshold, which represents the difference in stimuli that leads to a user correctly differentiating reference and test stimuli 75% of the time.

A one-up/one-down adaptive staircase method⁴⁸ was used for the experimental design. Each participant was presented with a reference stimuli, followed by a test stimuli that was the combination of the reference stimuli and a predefined step size. The participant then chose whether the two stimuli were the same or different. Upon responding that the stimuli were different, the step size between the reference and test stimuli was decreased by 10%. If, on the other hand, the participant responded that the stimuli felt the same, the step size was increased by 30%. This three-up/one-down weighting scheme results in a proportion correct values of 75%.

The adaptive staircase experiment was conducted for four total conditions: warming the entire thermal device, cooling the entire thermal device, warming a single row of the TEM array, and cooling a single row of the array. The bottom horizontal row of TEM elements in the device was chosen for the line conditions (Figure 3 (a-b)), which corresponds to testing the JND of the thenar eminence and base of the palm. The chosen conditions were selected to evaluate both the global and localized thermal sensitivity of the palm, as these areas are critical for perceiving thermal feedback in AR applications.

A reference stimulus of 4°C above or below the device's ambient temperature (30°C) was chosen for the heating and cooling trials, respectively. An initial step size of 4°C was chosen, meaning the initial test stimulus was 8°C above or below ambient conditions. Each stimuli was presented to the user for a period of 3.5 seconds, with no Inter-Stimulus Interval (ISI) between them (ISI=0s). No ISI was chosen to avoid time order errors, based on the results of Hojatmadani et al.⁴⁹, who found that ISI had a significant effect on calculated JNDs. Before and after the presentation of the two stimuli the thermal device was allowed to return to its ambient temperature. Each staircase test was conducted until 10 reversals were observed (changes in response from same to different or different to same, see Figure 3 (c)). The step sizes at the last eight reversals were then averaged to calculate the participant's JND for the specific condition.

The results of the JND testing (Figure 3). The individual JNDs for each condition failed to reject the null hypothesis of the Shapiro-Wilk test, indicating that they come from normal distributions. As such, the individual JNDs for each condition were fit to a normal curve in order to derive the 95% Confidence Interval (CI). The "Line-Warming" condition was found to have an average JND of 3.88°C (95% CI: 3.49°C-4.27°C), the "Line-Cooling" condition to have an average JND of 3.75°C (95% CI: 3.36°C-4.14°C), the "All-Warm" condition to have an average JND of 2.51°C (95% CI: 2.30°C-2.71°C), and the "All-Cool" condition an average JND of 2.88°C (95% CI: 2.54°C-3.22°C).

An ANOVA was run on all four conditions and no significant difference was found among the conditions ($p = 0.0549$). However, the low p value gives weight to the observed trend that the JND was smaller for the "All" mode conditions, implying that users can detect a smaller threshold between presented stimuli when the entire TEM array is activated.

2.5 Experiment 2: Temperature Passthrough

No matter the choice of body placement of an AR indirect thermal feedback device, there will be an occluded area of skin the user cannot use for sensing their physical environment. This experiment validates **DC 2: Temperature Passthrough** by characterizing the efficacy and immersiveness of our thermal device's "temperature pass-through" capability. We conducted an object interaction experiment utilizing a test stand with a temperature-controlled surface and virtual replicas of the test stand. The test stand's contact area was made from 6061 aluminum CNC'd into a concave ellipsoidal surface. An embedded thermistor in the aluminum enabled closed-loop temperature control using a 45mmx45mm TEM (ATS-TEC40-39-004) under the aluminum component. This assembly was then mounted onto a copper water-cooling heatsink for temperature management.

Participants were asked to compare the temperature of pairs of objects in a series of trials and to state whether the objects were at equal or different temperatures. Table 1 in Figure 4 describes the different comparisons that composed the series of trials. The "Real vs Virtual" trials asked participants to wear the device on their right hand and compare the test stand's temperature against its virtual replicas. The "Bare vs Device" trials involved just the physical test stand, with the comparison made by first touching the test stand with the bare left palm and then with our haptic device equipped on the right palm. We chose to ask participants to use their bare left hand to avoid the long delays associated with mounting/dismounting the thermal device on the right hand. Each trial was performed once with object temperatures above the participant's skin temperature ("Warm") and again with temperatures below skin temperature ("Cool"). The order in which each condition was tested was randomized between participants. At the end of this experiment, participants were asked to rate the overall realism of the object interactions during the AR experience using a Likert-scale of 1-7, with 1 being completely unrealistic and 7 being completely realistic.

To account for participant-level variation and within-subject temperature delta variation, a Generalized Linear Mixed Effects (GLME) model was used to predict response accuracy. Fixed effects included the warm vs cool condition, and the type of comparison being made (bare left hand + device right hand vs both with device right hand). Random effects were participant

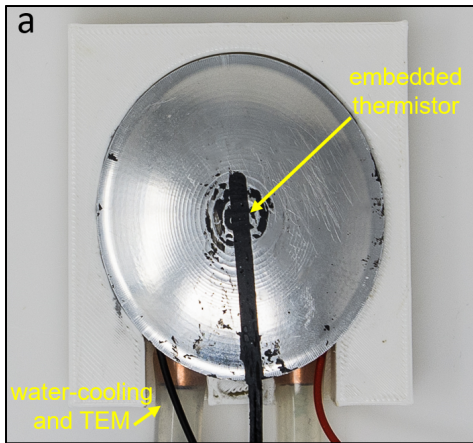


Table 1. Temperature passthrough test conditions.

Condition	Comparison Type	Temperature	# Trials
1	Real vs Virtual	Warm	3
2	Real vs Virtual	Cool	3
3	Bare vs Device	Warm	3
4	Bare vs Device	Cool	3
Total Trials Per Participant			12

Abbreviations

RV: Real vs Virtual
 BD: Bare vs Device
 W: Warm
 C: Cool

Table 2. GLME fixed effects summary.

Fixed Effect	Condition	Response Accuracy		$\beta_{\log\text{-likelihood}}$		p
		Mean (%)	95% CI	Mean	95% CI	
Base (Intercept)	RV-W	86.8	78.2 — 92.3	1.88	1.26 — 2.46	<0.001
Temperature	RV-C	82.3	60.1 — 93.23	-0.34	-0.83 — 0.15	0.169
Comparison Type	BD-W	77.8	54.0 — 91.3	-0.63	-1.11 — -0.14	0.012
Interaction Term	BD-C	80.0	33.6 — 96.9	0.47	-0.01 — 0.96	0.057

Figure 4. Temperature Passthrough Experimental Setup, Conditions, and Results.

(a) A convex aluminum surface with an embedded thermistor sits atop a thermoelectric module and heatsink to act as a temperature-controlled surface. (Table 1) Two conditions—the temperature of the surface relative to ambient and the method of comparison—were tested using a Generalized Linear Mixed Effects model (Table 2).

and temperature variation. A logit link function was employed as both predictors were ordinal. Significance of the Likert-scale realism score was tested using the Wilcoxon Sign Rank test. Post-hoc binomial tests were conducted to calculate response accuracy p-values.

Table 2 in Figure 4 shows the results of fitting the GLME model. Fixed effects showed that the warm vs cool condition had no significant effect on accuracy ($p = 0.169$), while the bare-handed vs purely haptic predictor was significantly associated with accuracy ($\beta_{\log\text{-likelihood}} = -0.625, p = 0.012$). This effect can be seen in its average response accuracies, with the overall accuracy of the haptic device at 84.6% ($p < 0.001$), and the bare-handed vs device accuracy of 78.9% ($p < 0.001$). Realism scores had an average value of 5.73 ($p < 0.001$), indicating that participants experienced a moderate degree of realism.

2.6 Experiment 3: Spatial Patterns

We developed a spatial pattern discrimination task for our participants to begin validating **DC 3: Spatiotemporal Patterns**. In this task, participants were presented with one pattern from a predefined set of 6 patterns: the left, right, or middle vertical column of the array, or the top, bottom, or middle horizontal row of the array. After a brief period of exposure, the pattern transitioned to another pattern from the set. Participants were asked to report noticing any change in the spatial profile of the thermal sensation applied to their palm. This process was conducted for every combination of pattern pairs from the set, for both warm and cool stimuli.

A temperature step size of 8°C above/below ambient was used for the presentation of thermal patterns. This was chosen to be well above the JNDs measured in the first experiment to ensure there were no difficulties in discriminating due to temperature differentials. Each pattern was applied to the participant for 3 seconds before transitioning to the second pattern for another 3 seconds, after which the thermal device returned to ambient skin conditions.

The results of the spatial pattern discrimination task are shown in Figure 5. Accuracy in detecting pattern changes ranged from 41.7% to 100% for warm stimuli and from 50.0% to 100% for cool stimuli. The warm stimuli condition had an overall probability to detect transition of 77.8%, while the cool stimuli condition had an overall probability to detect of 78.9%. There was no significant difference in responses between conditions ($p > 0.999$).

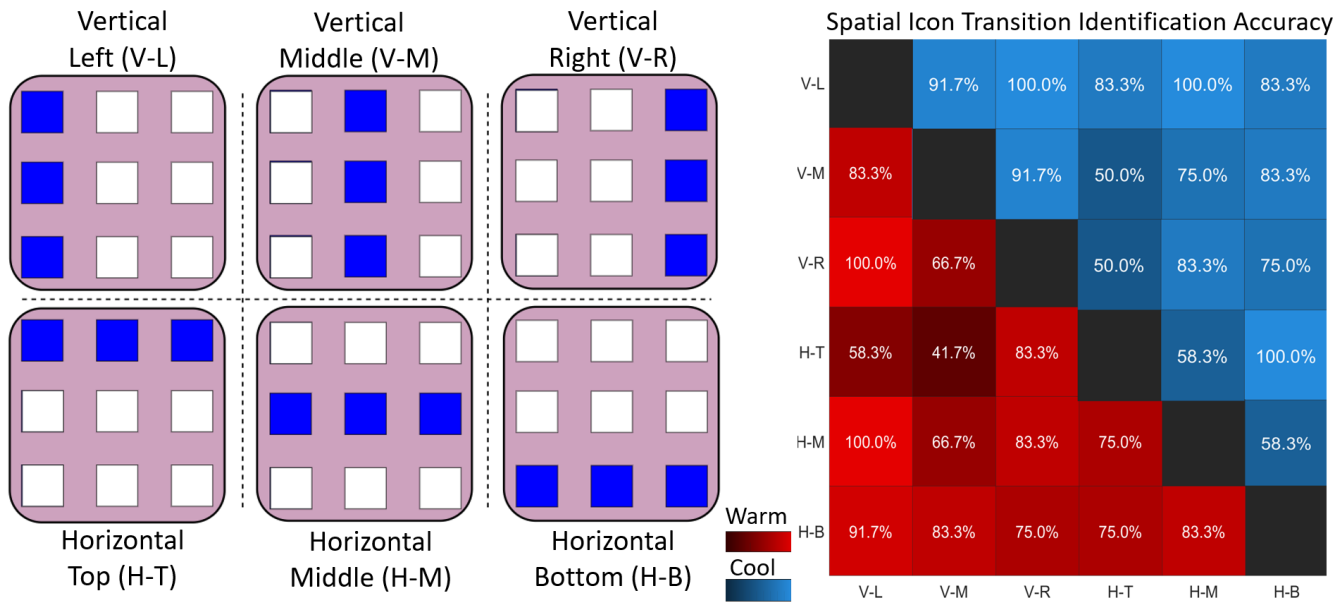


Figure 5. Experiment 3 Overview and Results.

Transitions between six spatial patterns that utilized the device’s 3x3 TEM grid were applied to participants wearing the device, for both warm and cool sensations. The reported discrimination accuracy for each pattern pair transition are shown in the matrix heatmap on the right.

2.7 Experiment 4: Moving Thermal Rendering in AR

The final experiment conducted was to evaluate the impact of **DC 3: Spatiotemporal Patterns** on immersion and the perception of a moving stimuli in AR. An application was developed in Unity for the HoloLens 2⁵⁰ wherein users viewed a small ball moving across a virtual surface (Figure 6 (a-c)). Participants were asked to place their palm down above a specified area of the surface while wearing the thermal device, and sequential singular TEMs in the device’s array were activated as the users received visual feedback of the ball rolling under their hand. This process was repeated for both warm and cold stimuli, and again with no thermal feedback.

A velocity of $3.5 \frac{m}{s}$ was chosen for the ball, as preliminary testing showed this was within the range of quick response times for the sequential activation of the TEMs. When thermal stimuli were applied, a step size of $\pm 10^\circ\text{C}$ above/below ambient skin conditions was chosen, again based on preliminary testing that showed consistent responses with this range.

After undergoing the AR experience with and without thermal feedback, participants were given a brief questionnaire regarding their experience. Participants were asked to rate their feeling of enjoyment and sense of immersion for both conditions using a Likert scale. Additionally, they were asked to rate the perceived realism of the moving thermal sensation when it was present. Finally, they were asked their preference in modality, with the options of: with thermal feedback, without thermal feedback, or no preference.

Figure 6 (d) shows the results of the questionnaire. Regarding feelings of enjoyment, without feedback had an average response of 3.42, while with feedback had a rating of 5.50. Sense of immersion without feedback averaged 3.08, and 5.67 when feedback was present. Participants rated the realism of the moving thermal sensation as 5.83. Not shown in Figure 6 is modality preference, as all participants indicated a preference for thermal feedback.

Wilcoxon Signed Rank tests were conducted comparing the two conditions for sense of enjoyment and immersion. Both metrics showed a significant increase in positive feelings with the presence of thermal feedback (both $p < 0.001$). A Signed Rank test was also conducted for the ratings of realism for the thermal sensation to see if there was any deviation from a mean of 4 (neutral feelings about realism). The results showed a significant difference ($p < 0.001$), indicating that the applied spatiotemporal patterns did elicit the perception of movement. Unsurprisingly, a binomial test found significance in favor of thermal feedback in regards to preference in modality ($p < 0.001$).

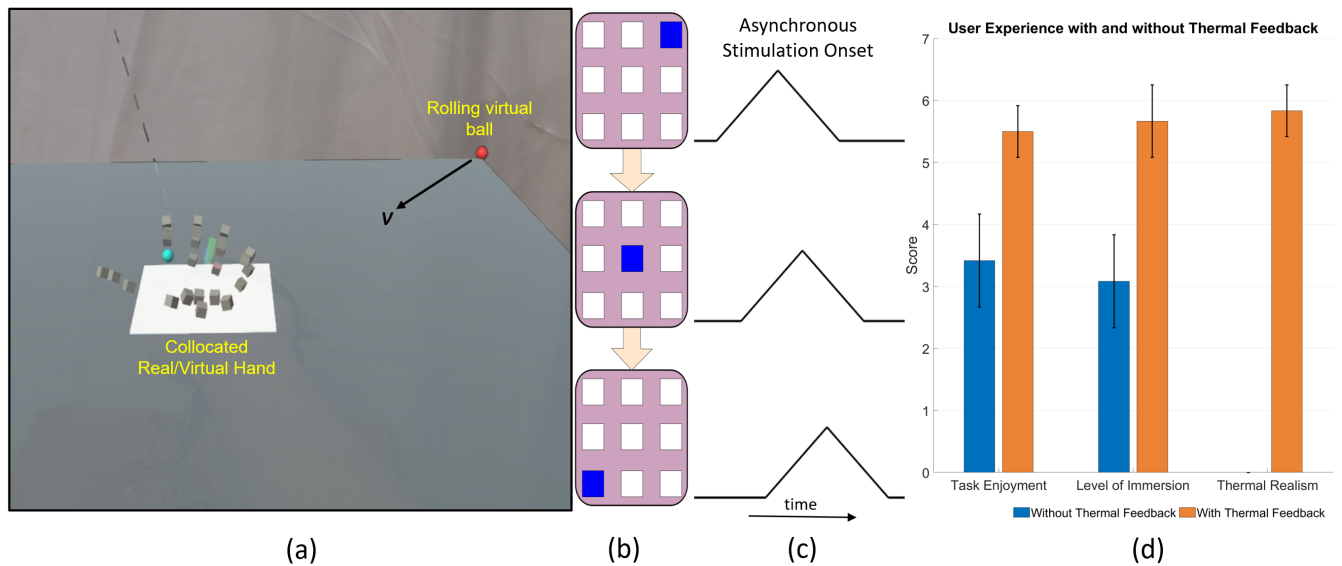


Figure 6. Experiment 4 Overview and Results.

(a) The AR application participants experienced while wearing the HoloLens 2. A red ball rolls with a velocity v across the gray and white squares while the participant holds their hand (equipped with the thermal device) above the white square. (b) Sequential thermal stimuli are applied asynchronously (c) to the palm to elicit the sensation of a moving thermal source as the ball moves over the white square. Qualitative Results (c) showed a consistent transition from negative to positive sentiment with the addition of thermal feedback.

3 Discussion

A set of design considerations for thermal feedback in MR/AR was developed by this work with the intent to promote the development of future thermal feedback devices for use in MR/AR experiences. A custom wearable thermal feedback device was created, and a set of four human subject experiments were performed that both demonstrated our haptic device satisfied these design considerations and that meeting the considerations resulted in an immersive experience for the user.

DC 1: Indirect Feedback was satisfied by our choice to place our device on the palm of the user. In conversation during and after the experiments, participants reported that discomfort from the device came mainly from the relatively short tether to its power supply and water reservoir. Only one participant felt the flexible device directly prevented them from naturally interacting the real and virtual objects utilized in our experiments. Our choice of targeting the palm showed no impact in the perception of thermal sensations, demonstrated by the JND calculations in Experiment 1. The warm and cold JNDs observed line up with those previously observed in literature for other parts of the body^{49,51}. This indicates that the device provides adequate thermal cues for humans to discriminate thermal stimuli without inhibition by the device itself, despite the utilization of small, low-powered thermal actuators.

The results of Experiment 2 support the idea that **DC 2: Temperature Passthrough** is an effective solution to compensating for the lack of direct physical contact on areas of the skin in use by a haptic device. The overall accuracy of the thermal device in distinguishing temperature differences between real and virtual objects was acceptable at 84.6%, indicating that the passthrough mechanism enables participants to perceive temperature cues with a moderate degree of fidelity. However, the reduced accuracy observed when comparing cooler objects while wearing the device, while not statistically significant, suggests that further refinement of the device's cooling performance is necessary. This limitation may be attributed to the slower response time of the thermoelectric modules when reaching cooler target temperatures compared to warmer ones (see the Methods section). Improving the cooling rate could help equalize performance across temperature ranges, further enhancing the passthrough capability. Additionally, the higher concentration of cool mechanoreceptors in the skin, and therefore higher sensitivity to cool sensations, could have allowed participants to more easily distinguish differences in presented thermal sensations.

The Bare vs Device condition revealed a statistically significant reduction in accuracy compared to bare-handed trials, with average accuracy dropping to 78.9%. This suggests that, while the passthrough mechanism is effective, it does not entirely replicate the natural tactile and thermal sensitivity of bare skin. Nonetheless, the realism scores reported by participants, averaging 5.73 on a 7-point Likert scale, indicate that the thermal feedback system still provides a moderately realistic and immersive experience.

The effectiveness of **DC 3: Spatio-Temporal Patterns** was validated through Experiments 3 and 4. In experiment 3, both

the individual thermal pattern transition detection accuracies and the overall detection accuracy are consistent with previous studies involving stationary thermal arrays^{29,52}. This implies the wearable device is able to display spatial cues to the user for use in user experience and interfaces beyond simply rendering bulk thermal properties of objects. This ability to spatially discriminate thermal patterns lends credence to the concept of activating singular portions of the TEM array to simulate small or irregularly shaped contact areas with a virtual object. For example, if a user were to touch their hand to a virtual cup halfway filled with a hot liquid, only the portion of the palm at the level of the liquid could be stimulated. The observation of moving thermal sensations and their positive effects on user experience was demonstrated by participant feedback in Experiment 4. The overwhelmingly positive results demonstrate the immersiveness of a thermal device that meets this design consideration. Participant feedback supports the idea of using spatial-temporal patterns to elicit a moving sensation for a thermal stimulus. To our knowledge, this is the first work that attempts to elicit such a sensation using only thermal input.

It is necessary to highlight the lack of portability of the current thermal device. Although wearable, the TEMs are connected by wires to the pcb control board. Additionally, the water cooling channels within the device is connected to a large reservoir. This limits the range of motion of the user to within a few feet of the tabletop where the pcb and water reservoir are located. Future work needs to address this lack of portability by designing a new prototype that relocated the control hardware onto the arm of the user. A novel solution would need to be developed to have portable water cooling, or alternative approaches to temperature management must be explored.

Another limitation in the device itself is the inconsistent application of uniform pressure for each TEM on the palm throughout the array. Attempts were made to allow the TEM array to contour to the palm by using a flexible silicone material and molding it to have a convex shape. Yet it is apparent by looking at the system response of individual TEMs (Figure 9 (d) and (e)) that not all TEMs exhibited the same thermal response times and damping/underdamping behavior when in contact with the palm. Contact pressure has long been known to affect thermal resistance between an object and human skin⁵³⁻⁵⁵. A variable contact pressure then affects the heat flow out of a TEM and into the surrounding skin. This means that a set of PID gains for temperature control for one set of TEMs will not be appropriate for another set with a different average contact resistance. A more efficient way of applying even contact pressure is needed, or a method of determining thermal contact resistance and adjusting individual PID gains accordingly.

In conclusion, the development and testing of a novel wearable thermal feedback device has contributed to our understanding of what additional design considerations are necessary to enhance user perception and immersion within mixed and augmented reality experiences. Despite some limitations related to sample size and uniform pressure application across the thermal elements, the results are promising and demonstrate an exciting avenue for further research and development. Moving forward, continued improvements to the device design and the identification of additional design considerations, alongside larger scale testing, are likely to further substantiate these findings and open up new uses for thermal feedback in MR/AR.

4 Methods

4.1 IRB Approval

This research study underwent ethical review and was approved by the appropriate Institutional Review Board (IRB) prior to its initiation. The purpose of the IRB review is to ensure the protection of human participants involved in the research and to ensure compliance with applicable ethical guidelines and regulations.

4.2 AR Hardware and Development Software

All AR testing was performed with the HoloLens 2 headset. The AR scenarios used in experiments 1 through 4 were developed using Unity 2020.3.34f1 and the Microsoft Mixed Reality Toolkit (MRTK) v2.8.3.

The thermal haptic device was fabricated using a three-layer silicone structure, each layer serving a specific function. The top layer, which made direct contact with the user's palm, was designed to accommodate the TEMs and heat sinks. The middle layer incorporated water channels for cooling the cold side of the TEMs and provided attachment points for the Velcro strap used to secure the device to the user's hand. The bottom layer provided space for wire management and included dedicated slots for the thermistors, which measured the temperature of the real-world objects with which the user interacted.

Each silicone layer was molded using two-part silicone and fabricated in a two-part 3D-printed mold. These layers were cast separately and bonded with silicone-compatible CA glue. The heatsinks were inserted into the slots in the top silicone layer and attached with CA glue, and the TEMs were attached to the heatsinks using thermally conductive putty. The same putty was also used to affix a thermistor on top of each TEM to provide control loop feedback. Thermistor slots were strategically positioned in the bottom layer directly below each TEMs to provide a one-to-one mapping of the TEMs with each external thermistor. This allowed the device to achieve "thermal passthrough" and pass on the temperature measured from the external object to the user's palm without loss of spatial resolution.

4.3 Thermoelectric Modules

A thermoelectric module, also known as a Peltier device, creates heat flux across the junction of two dissimilar materials. When a DC electric current flows through the device, a temperature differential arises across the module as heat is transferred from one side to another, creating a “hot” side and a “cold” side, shown in Figure 7 (a). The direction of heat flow is reversible by changing direction of current flow through the TEM, meaning that a single contact surface can be used for both heating and cooling an object. This is important to keep in mind as the terms “hot” and “cold” are used to reference specific surfaces of the TEM, regardless of the direction of the temperature gradient. Convention is to designate the temperature-controlled surface as the “cold” side, with the “hot” side then being used for thermal management.

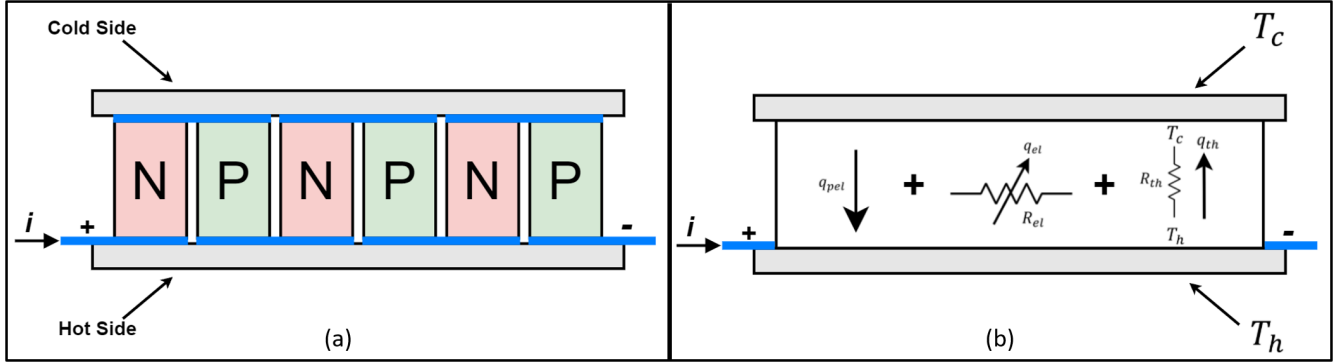


Figure 7. a) A thermoelectric device is made from alternating n- and p-type semiconductors placed in series electrically but in parallel thermally. When a DC current is passed through the semiconductors, a hot and cold side develop. b) This temperature differential is due to heat flow from the Peltier effect, q_{pel} , and is resisted by electrical waste heat generation, q_{el} , and natural heat conduction, q_{th} .

Heat absorption on the “cold” side of the device (q_{pel}) is a function of component materials, current temperature (T_c) and applied current (I):

$$q_{pel} = -\alpha T_c I \quad (1)$$

where α is the Seebeck coefficient of the device, a term that encapsulates material properties, and the negative sign represents heat flow *out* of the “cold” side. This heat absorption is impeded by two additional effects: natural heat conduction back to the “cold” side due to the temperature differential, and waste heat generated due to the device’s internal resistance and applied current.

Actual heat flow out of the “cold” side is more accurately described using the components of Figure 7(b) in the following equation:

$$q_c = -\alpha T_c I + \frac{1}{R_{th}} (T_h - T_c) + \frac{1}{2} R_{el} I^2 \quad (2)$$

where R_{th} and R_{el} represent the device’s thermal and electrical resistances, respectively. Only half of the electrical heat generated, $R_{el} I^2$, is included, as it is assumed waste heat is dumped equally on both sides of the module. The last two terms describing thermal conduction and waste heat have an important ramification: as the temperature differential across the device rises a decreasing amount of heat is effectively moved and the module becomes less efficient. There comes a point where natural heat conduction and waste heat generation completely negate the heat flow induced by the thermoelectric effect and the “cold” side temperature begins to rise, defining a maximum ΔT that can be generated across the device. If the “hot” side of the device is held near ambient conditions using a heat sink or other thermal management solution, this maximum temperature differential describes the bounds of simulated thermal sensations that can be applied to the skin contacting the device.

4.4 Control Architecture

Special consideration must be given to the control hardware used with a TEM. Voltage regulation using an H-Bridge circuit controlled with pulse-width modulation (PWM) has a negative impact on the TEM’s efficiency due to excessive waste heat generation. As described in (2), this is because the waste heat generated scales quadratically with applied current while thermoelectric heat flux is only linearly proportional to current. A PWM controller works by rapidly switching between a

constant DC voltage and a grounded input. This method works well for loads with an inductive component, such as a motor, as the resulting current across the load is effectively steady and scales with the PWM's duty cycle. A TEM, on the other hand, is a purely resistive load, meaning that the induced current rapidly switches between a max value and zero amps, amplifying the waste heat losses. The solution to this problem is to filter the TEM's power source to generate a variable DC voltage supply with as little ripple voltage as possible. This can be implemented using a differential filter or a class D amplifier, but is more easily achieved by utilizing off-the-shelf TEM drivers and additional passive components to complete the filtering circuit.

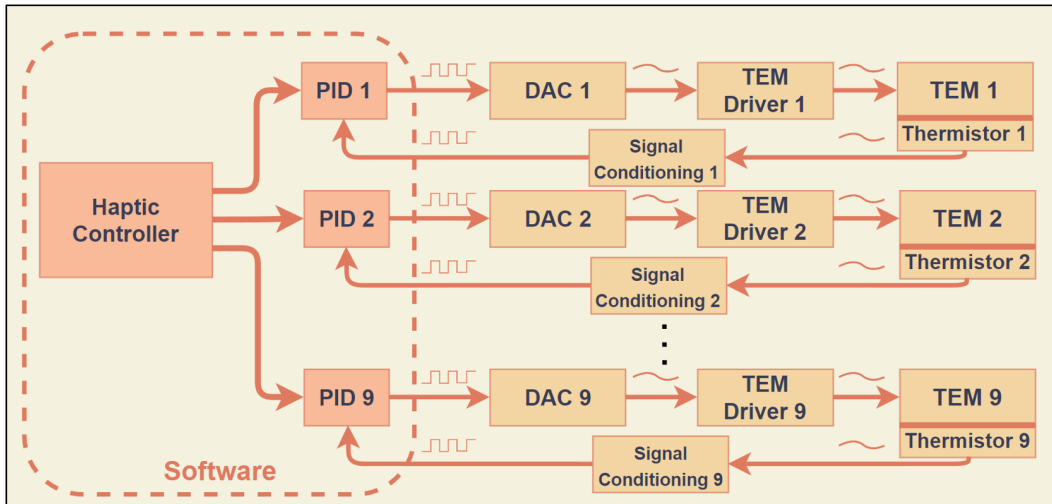


Figure 8. PID control signals are generated using a microcontroller and sent to digital-to-analog components to generate the control voltages necessary to drive each TEM. Thermistor readings are sent through signal conditioning and read by the microcontroller to close the loop.

The thermal display control loop we developed consist of a software PID controller, the ADN8833 TEM driver IC, a differential filter with a cutoff frequency of 5 kHz, and a thermistor mounted on the TEM's cold side for temperature feedback. While the drive circuit, filter, and temperature sensor are separate channels and contain unique hardware for each TEM, a single microcontroller is sufficient to run all the PID controllers and interface with a PC to receive thermal rendering input. This architecture is described in Figure 8. Additional components of the control PCB include separate multiplexers for the thermistor readings, TEM current sense, and TEM voltage sense, allowing each to be read by the microcontroller using a single input pin each.

4.5 Water Cooling

The fact that a TEM acts as a resistive load leads to a large amount of excess heat generation. In fact, the resistive heating dumped on the cold side ($\frac{1}{2}I^2R$) can sometimes approach Q_{max} , the maximum heat transfer capable by the TEM. Additionally, as described in equation 2, when in cooling mode natural thermal conduction within the TEM transfer heat from the hot side to the cold side. If not addressed, this heat buildup will quickly counter any attempts to lower the temperature of the TEM's cold side. To address this issue, we added aluminum heatsinks to the hot side of the TEM and implemented a novel watercooling solution to cool the heatsinks. Our solution is unique in that the water channels are built into the flexible and wearable silicone base itself, allowing for watercooling to be applied while still maintaining the mobile benefits of the wearable device already described. As seen in Figure 1 (c-d), each TEM assembly is watercooled in series, allowing for steady volumetric flow across each TEM.

When implementing the watercooling solution, it was first necessary to determine the maximum total energy transfer that the water cooling solution would need to handle. This maximum necessary heat dissipation occurs when the TEM is in cooling mode, meaning the cold side is reduced in temperature and the hot side is increased in temperature. Flipping the signs of the q_{pel} and thermal conduction components in equation 2, we arrive at the following equation describing heat flow into the hot side:

$$q_h = \alpha T_c I + \frac{1}{R_{th}} (T_c - T_h) + \frac{1}{2} R_{el} I^2 \quad (3)$$

As we are looking at the worst case scenario, we assume that $T_c = T_h$ and the thermal conduction component goes away. The first component, representing q_{pel} , can be set as the Q_{max} value of the specific TEM used. In our case, $Q_{max} = 1.7W$. The

maximum current for our TEM is 0.7A, and its resistive load is 4.17Ω. As there are nine total TEMs in our assembly, $Q_{maxArray}$ can be calculated as:

$$Q_{maxArray} = 9 * (1.7 + \frac{1}{2} * 4.17 * 0.7^2) = 24.49W \quad (4)$$

The maximum temperature rise for the water in the watercooling system can then be described by:

$$\Delta T = \frac{Q_{maxArray}}{\rho V c} \quad (5)$$

where ρ is the density of water ($1000 \frac{kg}{m^3}$), V is the volumetric flowrate (measured to be $2.25 \frac{ml}{s}$), and c is the specific heat of water ($4182 \frac{J}{kg \cdot K}$). Plugging these values in we get a maximum temperature differential of:

$$\Delta T = \frac{24.49}{1000 * 2.25E^{-6} * 4184} = 2.60K \quad (6)$$

The intermittent use of the TEMS, combined with relatively small ΔT for the water and the relatively large size of our water reservoir, leads us to conclude that the water cooling system will remain stable even with prolonged use of the device.

A heating element within the water reservoir kept the water temperature at 30°C, which is within the range of skin temperature of 25°C - 36°C^{1,56}. Due to the large size of the water cooling channels compared to the size of the device, and the thermal properties of the silicone material with which it was made, this maintained a steady temperature of 30°C for the entire thermal device. Maintaining the wearable thermal device at skin temperature is of great importance for multiple reasons. First and foremost, doing so establishes a neutral baseline, enabling the user to perceive both warming and cooling stimuli from the device. This neutral baseline also minimizes sensory adaptation, thereby preserving the sensitivity and responsiveness of the user's skin to the thermal haptic feedback. Additionally, keeping the device at skin temperature when not actively providing thermal feedback enhances user comfort and reduces the likelihood of skin irritation or discomfort from prolonged contact with a device that is either too cold or too warm.

4.6 Device Performance

The PID gains were tuned by hand, with the same gains applied to each TEM sub-system. Investigating the dynamic performance of the device, a step input exhibited a quick response for both warming and cooling modes while in contact with a human palm. A warming rise time of 1.4 seconds and a cooling rise time of 2.4 seconds were observed (Figure 9 (b-e)). It is worth noting that the disparity in these rise times can be ascribed to the resistive heating of the TEMs, which facilitates the temperature increase in warming mode while impeding the temperature decrease in cooling mode.

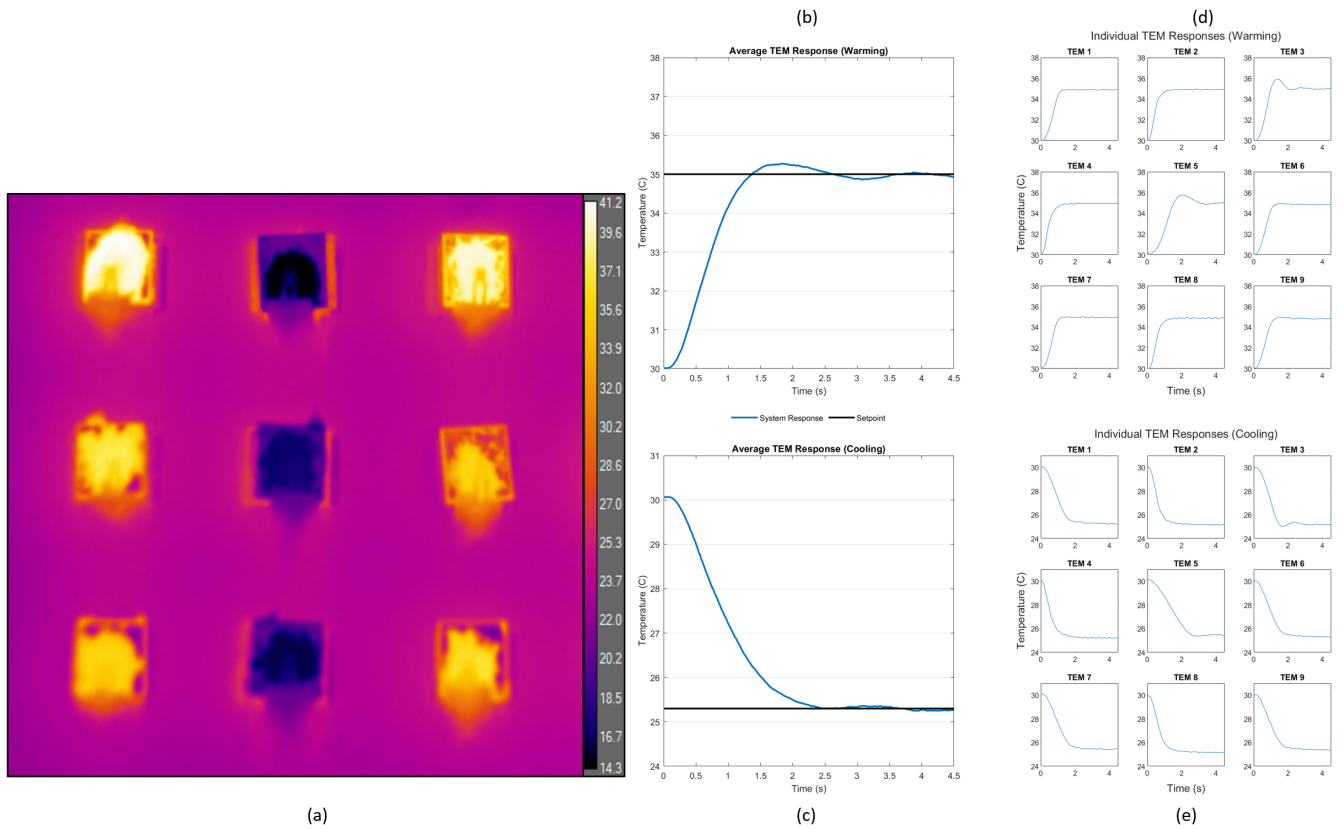


Figure 9. (a) Each channel of the TEM array can be individually actuated, allowing for multiple spatial patterns to be formed and presented to the palm. (b-c) Also shown in Figure 1(e). The average temperature response to a step input while in contact with a human palm for warming (b) and cooling (c) modes. (d-e) Individual TEM responses for warming (d) and cooling (e) show that variance exists in an individual TEM's response, most likely due to variable contact pressure with the palm (and therefore variable rates of thermal transfer into the skin).

References

1. Jones, L. A. & Berris, M. Material discrimination and thermal perception. *Proc. - 11th Symp. on Haptic Interfaces for Virtual Environ. Teleoperator Syst. HAPTICS 2003* 171–178, DOI: [10.1109/HAPTIC.2003.1191267](https://doi.org/10.1109/HAPTIC.2003.1191267) (2003).
2. Peiris, R. L., Peng, W., Chen, Z., Chan, L. & Minamizawa, K. ThermoVR: Exploring integrated thermal haptic feedback with head mounted displays. *Conf. on Hum. Factors Comput. Syst. - Proc.* **2017-May**, 5452–5456, DOI: [10.1145/3025453.3025824](https://doi.org/10.1145/3025453.3025824) (2017).
3. Gibbs, J. K., Gillies, M. & Pan, X. A comparison of the effects of haptic and visual feedback on presence in virtual reality. *Int. J. Human-Computer Stud.* **157**, 102717, DOI: [10.1016/j.ijhcs.2021.102717](https://doi.org/10.1016/j.ijhcs.2021.102717) (2022).
4. Lontschar, S., Deegan, D., Humer, I., Pietroszek, K. & Eckhardt, C. Analysis of Haptic Feedback and its Influences in Virtual Reality Learning Environments. In *2020 6th International Conference of the Immersive Learning Research Network (iLRN)*, 171–177, DOI: [10.23919/iLRN47897.2020.9155087](https://doi.org/10.23919/iLRN47897.2020.9155087) (2020).
5. John, B. & Wickramasinghe, N. A Review of Mixed Reality in Health Care. In Wickramasinghe, N. & Bendorff, F. (eds.) *Delivering Superior Health and Wellness Management with IoT and Analytics*, 375–382, DOI: [10.1007/978-3-030-17347-0_18](https://doi.org/10.1007/978-3-030-17347-0_18) (Springer International Publishing, Cham, 2020).
6. Santi, G. M., Ceruti, A., Liverani, A. & Osti, F. Augmented Reality in Industry 4.0 and Future Innovation Programs. *Technologies* **9**, 33, DOI: [10.3390/technologies9020033](https://doi.org/10.3390/technologies9020033) (2021).
7. Bazavan, L.-C., Roibu, H., Petcu, F. B., Cismaru, S. I. & George, B. N. Virtual Reality and Augmented Reality in Education. In *2021 30th Annual Conference of the European Association for Education in Electrical and Information Engineering (EAEEIE)*, 1–4, DOI: [10.1109/EAEEIE50507.2021.9531005](https://doi.org/10.1109/EAEEIE50507.2021.9531005) (2021).
8. Sırakaya, M. & Alsancak Sırakaya, D. Augmented reality in STEM education: A systematic review. *Interact. Learn. Environ.* **30**, 1556–1569, DOI: [10.1080/10494820.2020.1722713](https://doi.org/10.1080/10494820.2020.1722713) (2022).
9. Liberatore, M. J. & Wagner, W. P. Virtual, mixed, and augmented reality: A systematic review for immersive systems research. *Virtual Real.* **25**, 773–799, DOI: [10.1007/s10055-020-00492-0](https://doi.org/10.1007/s10055-020-00492-0) (2021).
10. Akgün, M. & Atıcı, B. The Effects of Immersive Virtual Reality Environments on Students' Academic Achievement: A Meta-analytical and Meta-thematic Study. *Particip. Educ. Res.* **9**, 111–131, DOI: [10.17275/per.22.57.9.3](https://doi.org/10.17275/per.22.57.9.3) (2022).
11. Guerra-Tamez, C. R. The Impact of Immersion through Virtual Reality in the Learning Experiences of Art and Design Students: The Mediating Effect of the Flow Experience. *Educ. Sci.* **13**, 185, DOI: [10.3390/educsci13020185](https://doi.org/10.3390/educsci13020185) (2023).
12. Milgram, P. & Kishino, F. A taxonomy of mixed reality visual displays. *IEICE TRANSACTIONS on Inf. Syst.* **77**, 1321–1329 (1994).
13. Azuma, R. T. A survey of augmented reality. *Presence: teleoperators & virtual environments* **6**, 355–385 (1997).
14. Hololens 2. <https://www.microsoft.com/en-us/hololens>.
15. Apple Vision Pro. <https://www.apple.com/apple-vision-pro/>.
16. Garcia-Valle, G., Ferre, M., Brenosa, J. & Vargas, D. Evaluation of Presence in Virtual Environments: Haptic Vest and User's Haptic Skills. *IEEE Access* **6**, 7224–7233, DOI: [10.1109/ACCESS.2017.2782254](https://doi.org/10.1109/ACCESS.2017.2782254) (2017).
17. Krogmeier, C., Mousas, C. & Whittinghill, D. Human–virtual character interaction: Toward understanding the influence of haptic feedback. *Comput. Animat. Virtual Worlds* **30**, e1883, DOI: [10.1002/cav.1883](https://doi.org/10.1002/cav.1883) (2019).
18. Richard, G., Pietrzak, T., Argelaguet, F., Lécuyer, A. & Casiez, G. Studying the Role of Haptic Feedback on Virtual Embodiment in a Drawing Task. *Front. Virtual Real.* **1** (2021).
19. Basdogan, C., Ho, C. H., Srinivasan, M. A. & Slater, M. An Experimental Study on the Role of Touch in Shared Virtual Environments. *ACM Transactions on Comput. Interact.* **7**, 443–460, DOI: [10.1145/365058.365082](https://doi.org/10.1145/365058.365082) (2000).
20. Slater, M. & Sanchez-Vives, M. V. From presence to consciousness through virtual reality. *Nat. Rev. Neurosci.* **6**, 332–339 (2005).
21. Ho, H. N. Material recognition based on thermal cues: Mechanisms and applications. *Temperature* **5**, 36–55, DOI: [10.1080/23328940.2017.1372042](https://doi.org/10.1080/23328940.2017.1372042) (2018).
22. Cai, S., Ke, P., Narumi, T. & Zhu, K. ThermAirGlove: A Pneumatic Glove for Thermal Perception and Material Identification in Virtual Reality. In *2020 IEEE Conference on Virtual Reality and 3D User Interfaces (VR)*, 248–257, DOI: [10.1109/VR46266.2020.00044](https://doi.org/10.1109/VR46266.2020.00044) (IEEE, 2020).

23. Lecuyer, A. *et al.* HOMERE: A multimodal system for visually impaired people to explore virtual environments. *Proc. - IEEE Virtual Real.* **2003-Janua**, 251–258, DOI: [10.1109/VR.2003.1191147](https://doi.org/10.1109/VR.2003.1191147) (2003).
24. Xu, J., Yoshimoto, S., Ienaga, N. & Kuroda, Y. Intensity-Adjustable Non-Contact Cold Sensation Presentation Based on the Vortex Effect. *IEEE Transactions on Haptics* **15**, 592–602, DOI: [10.1109/TOH.2022.3187759](https://doi.org/10.1109/TOH.2022.3187759) (2022).
25. Murakami, T., Person, T., Fernando, C. L. & Minamizawa, K. Altered touch: Miniature haptic display with force, thermal and tactile feedback for augmented haptics. *ACM SIGGRAPH 2017 Posters, SIGGRAPH 2017* DOI: [10.1145/3102163.3102225](https://doi.org/10.1145/3102163.3102225) (2017).
26. Osawa, Y. & Katsura, S. Rendering Thermal Sensation of Fingertip by Using Spatial Information of Heat Sources. *Proc. 2019 IEEE/SICE Int. Symp. on Syst. Integration, SII 2019* 620–625, DOI: [10.1109/SII.2019.8700450](https://doi.org/10.1109/SII.2019.8700450) (2019).
27. Aziz, K. M. A. *et al.* Haptic Handshank – A Handheld Multimodal Haptic Feedback Controller for Virtual Reality. In *2020 IEEE International Symposium on Mixed and Augmented Reality (ISMAR)*, 239–250, DOI: [10.1109/ISMAR50242.2020.00047](https://doi.org/10.1109/ISMAR50242.2020.00047) (IEEE, 2020).
28. Filingeri, D., Zhang, H. & Arens, E. A. Thermosensory micromapping of warm and cold sensitivity across glabrous and hairy skin of male and female hands and feet. *J. Appl. Physiol.* **125**, 723–736, DOI: [10.1152/jappphysiol.00158.2018](https://doi.org/10.1152/jappphysiol.00158.2018) (2018).
29. Zhang, J., Li, H., Song, A., Ding, Y. & Wu, J. Thermal Perception for Information Transmission: Theoretical Analysis, Device Design, and Experimental Verification. *IEEE Transactions on Haptics* **15**, 679–692, DOI: [10.1109/TOH.2022.3208937](https://doi.org/10.1109/TOH.2022.3208937) (2022).
30. Zhipeng, M. *et al.* A Thermal Tactile Display Device with Multiple Heat Sources. In *2012 International Conference on Industrial Control and Electronics Engineering*, 192–195, DOI: [10.1109/ICICEE.2012.58](https://doi.org/10.1109/ICICEE.2012.58) (2012).
31. Li, H. *et al.* Muscle Temperature Sensing and Control with a Wearable Device for Hand Rehabilitation of People After Stroke. In *2020 International Conference on Sensing, Measurement & Data Analytics in the Era of Artificial Intelligence (ICSMD)*, 94–99, DOI: [10.1109/ICSMD50554.2020.9261634](https://doi.org/10.1109/ICSMD50554.2020.9261634) (2020).
32. Kim, S. *et al.* Two-Dimensional Thermal Haptic Module Based on a Flexible Thermoelectric Device. *Soft Robotics* **7**, 736–742, DOI: [10.1089/soro.2019.0158](https://doi.org/10.1089/soro.2019.0158) (2020).
33. Bhatia, A., Hornbæk, K. & Seifi, H. Augmenting the feel of real objects: An analysis of haptic augmented reality. *Int. J. Human-Computer Stud.* **185**, 103244, DOI: [10.1016/j.ijhcs.2024.103244](https://doi.org/10.1016/j.ijhcs.2024.103244) (2024).
34. Lederman, S. J. & Klatzky, R. L. Hand movements: A window into haptic object recognition. *Cogn. Psychol.* **19**, 342–368, DOI: [10.1016/0010-0285\(87\)90008-9](https://doi.org/10.1016/0010-0285(87)90008-9) (1987).
35. Zhu, K., Perrault, S., Chen, T., Cai, S. & Lalintha Peiris, R. A sense of ice and fire: Exploring thermal feedback with multiple thermoelectric-cooling elements on a smart ring. *Int. J. Hum. Comput. Stud.* **130**, 234–247, DOI: [10.1016/j.ijhcs.2019.07.003](https://doi.org/10.1016/j.ijhcs.2019.07.003) (2019).
36. Peiris, R. L., Feng, Y.-L., Chan, L. & Minamizawa, K. ThermalBracelet: Exploring Thermal Haptic Feedback Around the Wrist. In *Proceedings of the 2019 CHI Conference on Human Factors in Computing Systems*, 1–11, DOI: [10.1145/3290605.3300400](https://doi.org/10.1145/3290605.3300400) (ACM, New York, NY, USA, 2019).
37. Manasrah, A., Crane, N., Guldiken, R. & Reed, K. B. Perceived Cooling Using Asymmetrically-Applied Hot and Cold Stimuli. *IEEE transactions on haptics* **10**, 75–83, DOI: [10.1109/TOH.2016.2578334](https://doi.org/10.1109/TOH.2016.2578334) (2017).
38. Jones, L. A. & Ho, H. N. Warm or cool, large or small? The challenge of thermal displays. *IEEE Transactions on Haptics* **1**, 53–70, DOI: [10.1109/TOH.2008.2](https://doi.org/10.1109/TOH.2008.2) (2008).
39. Caldwell, D. G., Tsagarakis, N. & Wardle, A. Mechano thermo and proprioceptor feedback for integrated haptic feedback. *Proc. - IEEE Int. Conf. on Robotics Autom.* **3**, 2491–2496, DOI: [10.1109/robot.1997.619335](https://doi.org/10.1109/robot.1997.619335) (1997).
40. Hirai, S. & Miki, N. A Thermal Tactile Sensation Display with Controllable Thermal Conductivity. *Micromachines* **10**, 359, DOI: [10.3390/mi10060359](https://doi.org/10.3390/mi10060359) (2019).
41. Lee, J. *et al.* Stretchable Skin-Like Cooling/Heating Device for Reconstruction of Artificial Thermal Sensation in Virtual Reality. *Adv. Funct. Mater.* **30**, 1909171, DOI: [10.1002/adfm.201909171](https://doi.org/10.1002/adfm.201909171) (2020).
42. Green, B. G. Localization of thermal sensation: An illusion and synthetic heat. *Percept. & Psychophys.* **22**, 331–337, DOI: [10.3758/BF03199698](https://doi.org/10.3758/BF03199698) (1977).
43. Liu, Y., Nishikawa, S., ah Seong, Y., Niiyama, R. & Kuniyoshi, Y. ThermoCaress: A Wearable Haptic Device with Illusory Moving Thermal Stimulation. In *Proceedings of the 2021 CHI Conference on Human Factors in Computing Systems*, 1–12, DOI: [10.1145/3411764.3445777](https://doi.org/10.1145/3411764.3445777) (ACM, New York, NY, USA, 2021).

44. Son, H., Wang, H., Singhal, Y. & Kim, J. R. Upper Body Thermal Referral and Tactile Masking for Localized Feedback. *IEEE Transactions on Vis. Comput. Graph.* **29**, 2211–2219, DOI: [10.1109/TVCG.2023.3247068](https://doi.org/10.1109/TVCG.2023.3247068) (2023).
45. Nakatani, M. *et al.* A Novel Multimodal Tactile Module that Can Provide Vibro-Thermal Feedback. In Hasegawa, S., Konyo, M., Kyung, K.-U., Nojima, T. & Kajimoto, H. (eds.) *Haptic Interaction*, Lecture Notes in Electrical Engineering, 437–443, DOI: [10.1007/978-981-10-4157-0_73](https://doi.org/10.1007/978-981-10-4157-0_73) (Springer, Singapore, 2018).
46. Israr, A. & Poupyrev, I. Tactile brush: Drawing on skin with a tactile grid display. In *Proceedings of the SIGCHI Conference on Human Factors in Computing Systems*, CHI '11, 2019–2028, DOI: [10.1145/1978942.1979235](https://doi.org/10.1145/1978942.1979235) (Association for Computing Machinery, New York, NY, USA, 2011).
47. Kenshalo, D. R., Holmes, C. E. & Wood, P. B. Warm and cool thresholds as a function of rate of stimulus temperature change. *Percept. & Psychophys.* **3**, 81–84, DOI: [10.3758/BF03212769](https://doi.org/10.3758/BF03212769) (1968).
48. Kingdom, F. & Prins, N. Adaptive Methods. In *Psychophysics: A Practical Introduction* (Elsevier Science & Technology), 2 edn.
49. Hojatmadani, M., Rigsby, B. & Reed, K. B. Time Delay Affects Thermal Discrimination. *IEEE Transactions on Haptics* **15**, 451–457, DOI: [10.1109/TOH.2022.3156122](https://doi.org/10.1109/TOH.2022.3156122) (2022).
50. Ungureanu, D. *et al.* HoloLens 2 Research Mode as a Tool for Computer Vision Research. *arXiv:2008.11239 [cs]* (2020). [2008.11239](https://arxiv.org/abs/2008.11239).
51. Kenshalo, D. R. Chapter 2 - BIOPHYSICS AND PSYCHOPHYSICS OF FEELING**Preparation of this chapter was assisted by USPHS Grant NS-02992 and NSF Grant GB-30610. In Carterette, E. C. & Friedman, M. P. (eds.) *Feeling and Hurting*, 29–74, DOI: [10.1016/B978-0-12-161922-0.50009-3](https://doi.org/10.1016/B978-0-12-161922-0.50009-3) (Academic Press, 1978).
52. Yang, G.-H., Kyung, K.-U., Srinivasan, M. & Kwon, D.-S. Quantitative tactile display device with pin-array type tactile feedback and thermal feedback. In *Proceedings 2006 IEEE International Conference on Robotics and Automation, 2006. ICRA 2006.*, 3917–3922, DOI: [10.1109/ROBOT.2006.1642302](https://doi.org/10.1109/ROBOT.2006.1642302) (2006).
53. Chen, F., Nilsson, H. & Holmér, I. Finger cooling by contact with cold aluminium surfaces — effects of pressure, mass and whole body thermal balance. *Eur. J. Appl. Physiol. Occup. Physiol.* **69**, 55–60, DOI: [10.1007/BF00867928](https://doi.org/10.1007/BF00867928) (1994).
54. Rykaczewski, K. Modeling thermal contact resistance at the finger-object interface. *Temperature* **6**, 85–95, DOI: [10.1080/23328940.2018.1551706](https://doi.org/10.1080/23328940.2018.1551706) (2019).
55. Tiest, W. M. An experimentally verified model of the perceived 'coldness' of objects. *Proc. - Second. Jt. EuroHaptics Conf. Symp. on Haptic Interfaces for Virtual Environ. Teleoperator Syst. World Haptics 2007* 61–65, DOI: [10.1109/WHC.2007.21](https://doi.org/10.1109/WHC.2007.21) (2007).
56. VERRILLO, RONALD., BOLANOWSKI, STANLEY., FRANCIS, CHRISTINE. & McGLONE, FRANCIS. Effects of hydration on tactile sensation. *Somatosens. & Mot. Res.* **15**, 93–108, DOI: [10.1080/08990229870826](https://doi.org/10.1080/08990229870826) (1998).

Acknowledgements

We gratefully acknowledge the support provided for this research by the National Science Foundation under the award 2225890. We also thank the volunteers and the participants who agreed to be part of the experiments. The content is solely the responsibility of the authors and does not necessarily represent the official views of the National Science Foundation.

Author contributions statement

A.W, R.G, and N.S conceptualized and designed the research. A.W., E.C., and R.G. designed and built the experimental hardware and conducted the experiment. A.W. and N.S analyzed the data. A.W. wrote the manuscript and prepared figures. All authors reviewed the manuscript.

Additional information

Competing interests The authors declare no competing interests.

Data Availability Data is available at <https://github.com/VU-RASL/ThermalFeedbackForAR-Data>